ISSN (Print) 1226-1750
ISSN (Online) 2233-6656
Journal of Magnetics 19(2), 146-150 (2014) http://dx.doi.org/10.4283/JMAG.2014.19.2.146

Comparison of Transverse Flux Rotary Machines with Different Stator Core Topologies

Jiyoung Lee[1]*, Shiuk Chung[1], Daehyun Koo[1], and Choongkyu Han[2]

[1]Korea Electro-technology Research Institute, Changwon, Gyeongnam 641-120, Korea
[2]Agency for Defense Development (ADD), Daejeon 305-152, Korea

(Received 6 January 2014, Received in final form 15 April 2014, Accepted 17 April 2014)

The objective of this paper is to provide a comparison between two transverse flux rotary machines (TFRM) with different topologies of stator cores. Depending on how to make stator core with laminated steel sheets, the one topology is 'perpendicular stacking core' and the other is 'separated core.' Both of the two cores have been designed considering 3-dimensional (3-D) magnetic flux path with the same output power conditions, but the core losses are quite different and it causes different magnetic and thermal characteristics. For comparison of these two topologies of stator cores, therefore, core losses have been calculated and used as a heat source in no-load conditions, and the thermal stress has been also calculated. 3-D finite element method has been used for the magnetic field, thermal, and stress analysis to consider the 3-D flux path of the TFRM. After comparing the analysis results of the two topologies, experimental results are also presented and discussed.

Keywords : core loss, finite element method, thermal analysis, thermal stress, transverse flux machine

1. Introduction

Since Transverse Flux Rotary Machines (TFRM) have a 3-dimensional (3-D) magnetic flux path, either the stator or the rotor has to be skewed for smooth operation [1-3]. Fig. 1(a) shows a typical TFRM, which has been studied at the Korea Electro-technology Research Institute. The stator is divided into an inner core, and an outer one. The outer core is divided again into upper and lower parts; and the lower part is shifted by a half pole-pitch with respect to the upper part, to create a skewing effect [1]. Initially, all cores of the rotor and stator were made of soft magnetic composite (SMC); but the stator core material has since been changed to laminated silicon steel, in order to improve its magnetic characteristics. However, although the laminated directions of the inner and outer cores are perpendicular to each other, with regard to the 3D magnetic flux path, the electro-magnetic force (EMF) increases non-linearly with the frequency [1], and the stator core surface temperature increases rapidly, even in no-load conditions. The reason that the EMF increases non-linearly with the frequency is because of eddy current losses, which process has been verified in [2]. To solve this problem, slits on the outer core have been suggested in [2], and here, another topology of stator is investigated. In this paper, the typical stator is called M1, which has a perpendicular stacking core; and the other stator is called M2, which has a separated core, as shown in Fig. 1. The perpendicular stacking core is made of two parts of cores, whose stacking directions are perpendicular to each other; while the separated core is made of bent core pieces, with only one stacking direction circumferentially. Except for the stator configuration, all the other conditions are the same.

The TFRMs with these two topologies of stator have been studied for high-torque direct-drive motor applications. The efficiency of a motor is important for effective direct drive motor systems; but more importantly, the total system, including the cooling system, should be compact, and have high efficiency. Reducing heat sources is one way of achieving high efficiency of both the motor, and the total system. In the TFRM, the number of poles is high, and the cores are highly saturated, so core loss is one of the major heat sources.

This paper discusses the severity of the loss and thermal problems with comparison of M1 and M2 through analysis and experiments. For the two topologies of stators, core losses are calculated and used as a heat source in no-load

*Corresponding author: Tel: +82-55-280-1416
Fax: +82-55-280-1490, e-mail: jylee@keri.re.kr

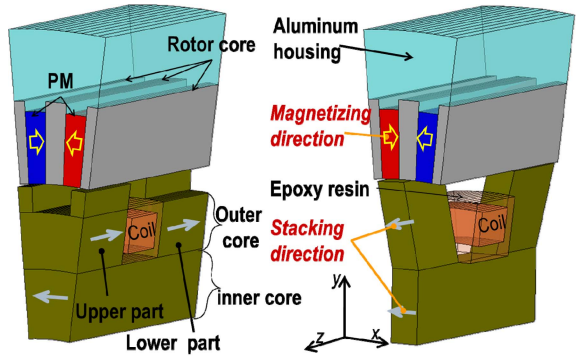

(a) M1 : perpendicular stacking core (b) M2 : separated core

Fig. 1. (Color online) Partial schematic illustrations of two analysis models with different stator configurations.

conditions, and the thermal stress has been also calculated. 3-D finite element method (FEM) has been used for the magnetic field, thermal, and stress analysis to consider the 3-D flux path of the TFRM. After comparing the analysis results of the two topologies, experimental results are also presented and discussed.

2. Analysis Models and Methods

In this section, the analysis models and analysis methods are introduced. Methods of heat source calculation, thermal analysis, and thermal stress analysis are also presented according to analysis procedure.

2.1. Analysis Model

Table 1 shows the common specifications of the TFRMs with stators M1 and M2. The total conceptual configuration of the TFRM is shown in another study [1]. For the analysis modeling of TFRM, one phase is enough because each phase is independent, and there is no mutual inductance. In addition, the analysis model is reduced by periodic conditions. The TFRMs have 2 phases and 60 poles/phase, so Fig. 1 shows the 1/60 configurations of the TFRMs.

Table 1. Common specifications of the TFRMs.

Contents	Value	Unit
Rated power	1.3	kW
Rated/max speed	250/300	rpm
Rated/max torque	50/75	Nm
Rotor diameter	206	mm
Rotor axial length	156	mm
Air-gap length	0.5	mm
No. of poles	60	Pole/phase
No. of phase	2	phase
No. of turn	90	Turn/phase
Stator core material	S23 (laminated silicon steel)	
PM material	NdFeB-N38UH (Br = 1.23T, Hc = –964 kA/m)	
Rotor core material	SMC : Somaloy 700	
Housing material	Aluminum 7075	

2.2. Heat Source Calculation

The EMF of the TFRM with M1 increases non-linearly with the frequency increase, as mentioned. This means that the core loss is severe in the machine, and it can cause thermal problem. In no-load condition, therefore, core loss is only treated here as a heat source. The other sources such as copper loss, magnet loss, and bearing loss are not considered. Furthermore, only the stator core loss is considered to clearly compare M1 and M2 because the rotor is the same.

The general three-term core loss model that is used to calculate the total core loss Pv in W/kg for a sinusoidal magnetic field is expressed as follows [4]-[6]:

$$Pv = Ph + Pc + Pe$$
$$= K_h \times f \times (B_m)^n + K_c \times (f \times B_m)^2 + K_e \times (f \times B_m)^{1.5} \quad (1)$$

where B_m is the peak value of the AC flux density, f is the frequency, K_h and n are the hysteresis core loss coefficients, K_c is the eddy-current core loss coefficient, and K_e is the excess core loss coefficient. The value of n=2 has been reported irrespective of the electrical steel used and will therefore be adopted for this analysis [5]. Then, (1) can be rewritten with a two-term core loss model as follows [6]:

$$Pv = K_1 B_m^{\,2} + K_2 B_m^{\,1.5}$$
$$K_1 = K_h \times f + K_c \times f^2,\ K_2 = K_e \times f^{1.5} \quad (2)$$

In this paper, core loss coefficients K_h, K_c, and K_e are

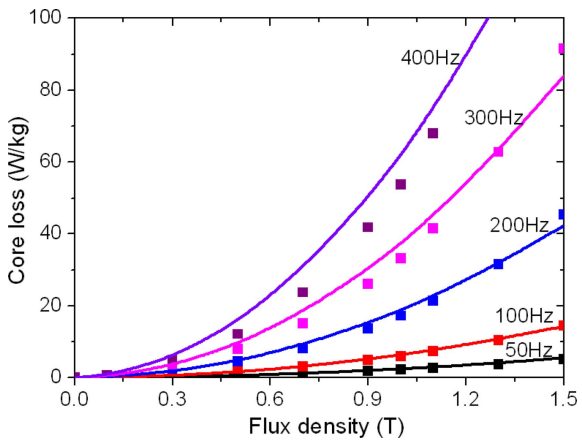

Fig. 2. (Color online) Core loss data of S23 (squares: measured data, lines: assumed data for analysis).

treated as constant values irrespective of frequency and flux density variation, and the coefficients are obtained by curve fitting the measured core loss data, as shown in Fig. 2. A previous core loss method [7] can be used for more accurate analysis, but this simple method using (1) and constant coefficients is used to reduce analysis time. The little error between the assumed and measured data as shown in Fig. 2 can be neglected, because the main object is the comparison of M1 and M2. For stator core material S23, the calculated coefficients are $K_h = 259.6$, $K_c = 2.35$, and $K_e = 0$, where the core loss is in units of W/m^3, and the mass density is 7750 kg/m^3.

2.3. Thermal Analysis

3-D FEM is used to analyze the temperature distribution in this paper. The heat transferred by radiation is ignored. The partial differential equation of the heat conduction and convection is expressed as:

$$\rho c\left(\frac{\partial T}{\partial t} + \{V\}^T\{L\}^T\right) = \{L\}^T([D]\{L\})T + Q \tag{3}$$

where ρ(kg/m^3) is the mass density, c(J/kg°C) is the specific heat, T(°C) is the temperature, t(s) is the time, $\{V\}$ is the velocity vector for mass transport of heat, $\{L\}$ is the vector operator, $[D]$ is the conductivity matrix, and Q[W/m^3] is the heat generation rate per unit volume. For steady-state analysis, the first term on the left-hand side of (3) is zero [8].

Newton's convection boundary condition is:

$$q_n = \alpha(T - T_{amb}) \tag{4}$$

where q_n is the heat flux. The heat flux flowing through the boundaries to its surroundings is described with the heat-transfer coefficient and the external temperature T_{amb}. For the analysis models, the convection boundary conditions are considered between stator teeth surfaces and inner air in the air gap, between the magnet and inner air, between the rotor core and inner air, and between the housing and outer air.

The convection heat transfer to the surroundings is dependent on the geometry and the cooling conditions. The convection coefficient is determined by two main quantities: 1) the ruggedness of the rotor and stator surfaces and 2) the peripheral speed of the rotor surface [8]. Since the TFRM is an outer rotor type, and the rotor housing has a smooth surface, an experiential formula [8] was used for calculation of the convection coefficient between the housing and outer air as follows:

$$h_\delta = 28(1 + \omega_\delta^{0.5}),\ \omega_\delta = \sqrt{(0.5v_r)^2 + v_a^2} \tag{5}$$

where v_r and v_a are the peripheral and axial velocities of the rotor surface, respectively.

The other convection coefficients on the surface in the air gap are calculated by an equation from a previous study [9], because the stator has a toothed structure:

$$h = \frac{6.6 \times v_{rr}^{0.67}}{10^5 \times l_g^{0.33}}\ (\text{W/cm}^2\cdot{}^\circ\text{C}) \tag{6}$$

where v_{rr} is the velocity of the air (cm/s), and l_g is the length of the air-gap (cm). The thermal conductivities of each material in the analysis model and the calculated convection coefficients are listed in Table 2.

Table 2. Thermal constant and coefficient.

Contents and Unit	Material	Value
Thermal conductivity (W/m°C)	Silicon steel	50
	SMC	20
	Copper	380
	Magnet	9
	Epoxy resin	0.15
	Aluminum	130
Convection coefficient (W/m^2 °C)	Housing outside	53
	Air-gap side	67

2.4. Thermal Stress Analysis

The stress analysis uses the quadratic hexahedral elements and the same mesh as in the thermal field analysis. Using Hooke's law, the stresses in an element are given by:

$$\sigma = D_e \cdot \{B_s \cdot \delta - \varepsilon_0\} \tag{7}$$

Where σ is a stress, D_e is the element elasticity matrix, B_s is the element strain matrix, is the global displacement vector, and is the element thermal strain matrix [10].

For the boundary conditions in the x, y, and z directions, it is assumed that the stator and rotor cores are completely fixed at the axis surface, and the displacements on the axial direction (z-direction) are zero.

Table 3 shows the Young's modulus (modulus of elasticity) and Poisson's Ratio of each material in the analysis

Table 3. Young's modulus and Poisson's ratio.

Material	Young's Modulus (10^9 Pa)	Poisson's Ratio
Silicon steel (RD/TD*)	200/210	0.27/0.3
Copper	110	0.34
Magnet	153	0.24
Epoxy resin	20.7	0.30
Aluminum	71.7	0.33

*RD and TD represent the rolling and transverse directions, respectively.

Table 4. Tensile strength and elongation

Material	Tensile strength (N/mm^2)	Elongation (%)
Silicon steel (RD/TD)	395 / 405	37 / 39
SMC	500	4

model. All values except the SMC can be obtained from general material information [11, 12]. For the precision value, however, 50PN600 in POSCO grade (50A600 in JIS, M600-50A5 in EN10106) is considered as silicon steel, and the average of values of rolling direction (RD) and transverse direction (TD) is used for analysis. In the case of SMC, the main ingredient of SMC is the same as silicon steel, but it is more like brittle material rather than ductile material because of sintering process of iron base powders. Somaloy 550 in Höganäs grade is considered for mechanical property of SMC, and the information is limited to tensile strength and elongation, which are compared with those of silicon steel in Table 4.

3. Analysis and experimental results

3.1. Analysis Results

In transient electro-magnetic analysis for core loss calculation, it uses quadratic tetrahedron and about 0.6 million elements. The analysis condition is that rotating speed is 300 rpm and input current is zero. Stacking direction and skin depth is also considered. In the aligned position between rotor pole and stator tooth, the flux density distributions of the two models are shown in Fig. 3. The cross section of flux path in M2 is smaller than that of M1, and so the flux density of M2 is higher on average. Fig. 4 shows the flux linkage in the coil and core losses calculated with magnetic analysis results. Although

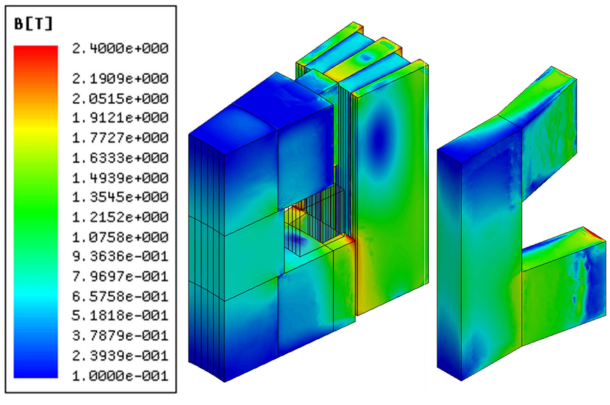

(a) M1 (b) M2

Fig. 3. (Color online) Flux density distribution after magnetic field analysis.

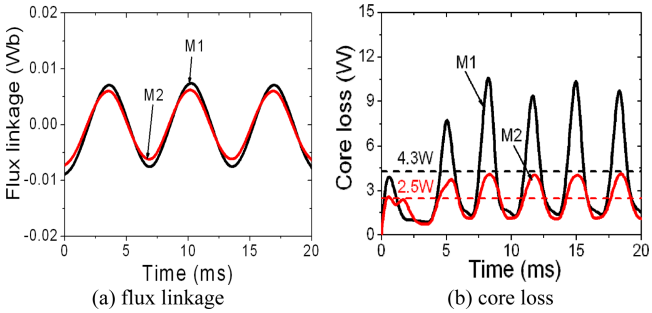

(a) flux linkage (b) core loss

Fig. 4. (Color online) Comparison of flux and core loss values for analysis models (no-load condition at the speed of 300 rpm).

all analysis conditions are the same, the flux linkage of M2 is slightly smaller than that of M1 because of stator cross section different. In the core loss comparison, however, the difference is bigger. When the core loss waveform reaches steady state, the average core loss value of M2 is as 1.7 times small as the value of M1. This average core loss is used as heat source of each stator.

The steady-state thermal analysis results are shown in Fig. 5. The temperature difference of the two models is big not only because core loss of M2 is smaller than that of M1, but also because the teeth surface area of M2 is

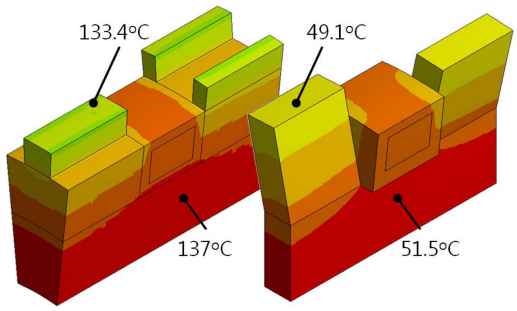

(a) M1 (b) M2

Fig. 5. (Color online) Temperature distribution after steady state thermal analysis.

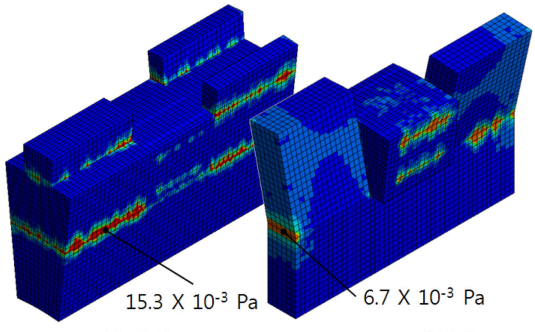

(a) M1 (b) M2

Fig. 6. (Color online) Equivalent stress distribution of the meshed model after static structural analysis.

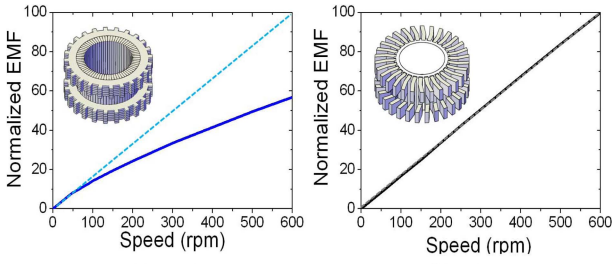

Fig. 7. (Color online) Normalized EMF according to rotor speed (dotted line : ideal curve, solid line : measured data).

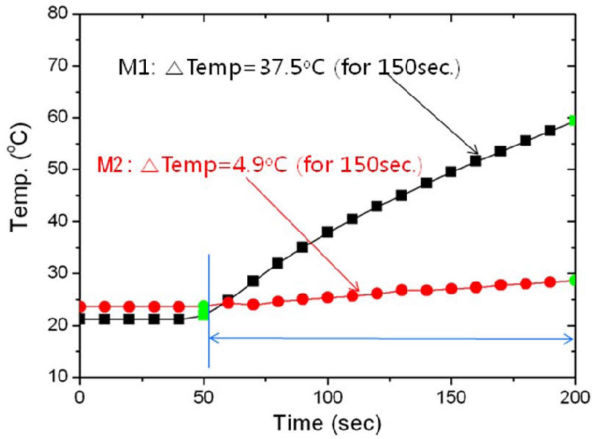

Fig. 8. (Color online) Measured temperature on stator tooth of each model (no-load condition at the speed of 300 rpm).

wider and so that heat radiates easily. These thermal distributions are used as sources of static structural analysis to calculate thermal stress.

Fig. 6 shows the equivalent stress distribution after static structural analysis. The absolute quantity is too small to have influence on structural problem, but it is clear that the equivalent stress of M2 is much smaller than stress of M1.

3.2 Experimental Results

It is difficult to measure only the stator core loss because the mechanical loss and rotor loss should be separated from the total losses. Therefore, the core losses of M1 and M2 are compared indirectly through EMF comparison. The non-linearly increasing EMF waveform, which has been mentioned as a problem of M1improved, is completely improved in M2, as shown in Fig. 7. Furthermore, it is clearly shown in Fig. 8 that the temperature differences of the stator tooth surface of each model are much higher than expected with the analysis results.

4. Conclusions

The core losses of topology M1 were very severe, based on analytic results, and the EMF test results. The characteristics of TFRM with M2, however, were certainly improved, because of the difference in quantity of the heat source, and structural differences for heat radiation. This is because the configuration of separated core has the same effect as that of the slits in [2], and the core losses were reduced, including eddy current loss. This has been proven, both analytically and experimentally. If laminated steel sheets are used for TFRM, the topology M2 should be used for the stator core, to reduce core losses, and to obtain the proper magnetic characteristics.

Acknowledgement

This work was supported by the Next Generation Military Battery Research Center program of Defense Acquisition Program Administration and Agency for Defense Development

References

[1] J. Y. Lee, S. R. Moon, D. H. Kang, and J. P. Hong, Proceedings of the 17th Conference on the Computation of Electromagnetic Fields (COMPUMAG) (2009).
[2] J. Y. Lee, D. H. Koo, K. H. Kang, and J. P. Hong, J. Magn. **17**, 51 (2012).
[3] J. Y. Lee, J. W. Kim, B. C. Woo, S. H. Lee, and J. P. Hong, Proceedings of the 17th Conference on the Computation of Electromagnetic Fields (COMPUMAG), (2009).
[4] F. Deng, IEEE Trans. Energy Conversion **14**, 1391 (1999).
[5] M. J. Manyage and P. Pillay, 42nd IAS Annual Meeting 1560 (2007).
[6] Maxwell Online Help, Ansoft Corporation, http://www.ansoft.co.kr/.
[7] J. Y. Lee, J. W. Kim, S. R. Moon, J. H. Chang, S. U. Chung, D. H. Kang, and J. P. Hong, IEEE Trans. Magn. **45**, 1776 (2009).
[8] Y. Huang, J. Zhu, and Y. Guo, IEEE Trans. Magn. **45**, 10 (2009).
[9] Y. G. Guo, J. G. Zhu, and W. Wu, IEEE Trans. Magn. **41**, 2124 (2005).
[10] Y. J Liu, Y. S. Lee, H. K. Jung, S. Y. Hahn, J. H. Youn, K. W. Kim, J. L. Kwon, D. J. Bae, and J. I. Lee, IEEE Trans. Magn. **36**, 1394 (2000).
[11] Efunda, http://www.efunda.com/home.cfm
[12] Matweb, http://www.matweb.com/search/MaterialGroupSearch.aspx